

Compact and Wide Upper-Stopband Triple-Mode Broadband Microstrip BPF

Wen Chen*, Yongjiu Zhao, ZhouxiaoJun

College of Electronic and Information Engineering, Nanjing University of Aeronautics and Astronautics,
Nanjing, China
e-mail: wen_011@126.com*

Abstrak

Sebuah tapis lolos tengah mikrostrip (BPF) dengan ukuran yang kompak, tepi tajam dan kinerja pita-henti-atas lebar menggunakan resonator terpotong mode rangkap tiga diusulkan. Resonator ini dapat membangkitkan satu mode ganjil dan dua mode genap pada pita lolos yang diinginkan. Karena peniadaan sinyal jalur utama, dua nol transmisi T_{z1} , T_{z2} dapat dibuat dekat tepi pita lolos untuk mencapai tepi yang tajam. Dua nol transmisi T_{z4} , T_{z5} diciptakan antara dua frekuensi harmonik h_{m2} dan h_{m3} dengan potongan terbuka dilipat dan garis-garis kopling interdigita. Karena kopling beban-sumber, satu nol T_{z3} diperkenalkan untuk memperdalam pita-henti. Sementara itu, nol T_{z1} digeser ke frekuensi cut-off yang lebih rendah dan tiga lainnya T_{z2} , T_{z4} , T_{z5} dapat sedikit diubah untuk menekan tiga frekuensi harmonik h_{m1} , h_{m2} , h_{m3} . Salah satu purwarupa tapis dengan lebar-pita kecil 34% dirancang, dibuat dan diukur.

Kata kunci: BPF, kompak, mode rangkap tiga, pita-henti-atas lebar, pita-lebar

Abstract

A broadband microstrip bandpass filter (BPF) with compact size, sharp skirt and wide upper-stopband performance is proposed using the triple-mode stub-loaded resonator. The resonator can generate one odd mode and two even modes in the desired passband. Due to the main path signal counteraction, two transmission zeros T_{z1} , T_{z2} can be created near the passband edge to achieve sharp skirt. Two transmission zeros T_{z4} , T_{z5} are created between two harmonic frequencies h_{m2} , h_{m3} by the folded open stub and the interdigital coupling feeding lines, respectively. Owing to the source-load coupling, one zero T_{z3} is introduced to deepen the stopband. Meanwhile, the zero T_{z1} is shifted to the lower cut-off frequency and the other three ones T_{z2} , T_{z4} , T_{z5} can be slightly turned to suppress three harmonic frequencies h_{m1} , h_{m2} , h_{m3} . One filter prototype with the fractional bandwidth 34% is designed, fabricated and measured.

Keywords: BPF, broadband, compact, triple-mode, wide upper-stopband

1. Introduction

High-performance wideband and broadband bandpass filters with the characteristics of compact size, wide stopband and high selectivity are essential for modern communication systems [1]. Especially, excellent upper-stopband performance is highly demanded for a wideband and broadband BPF to suppress the unwanted interference or noise [2]. In response to this need, numerous researchers have proposed various wideband and broadband BPFs with wide upper-stopband suppression [3-5]. In [3], a wideband BPF with wide upper-stopband is given using stepped-impedance cascaded 180° hybrid rings. Nevertheless, the designed BPF suffers from large size with complicated implementation. In [4], a compact wideband microstrip BPF is realized using a transversal resonator. By means of introducing asymmetrical interdigital coupled lines, five transmission zeros are generated in the stopband, and the upper-stopband extends to $2.5f_0$. A more compact and simple wideband BPF with the total size of $0.46\lambda_g \times 0.38\lambda_g$ is presented in [5] to obtain 30dB rejection level in the stopband from $1.2f_0$ to $3.8f_0$. Nevertheless the bandwidths in [4] and [5] are inconveniently adjusted. Recently, some multiple-mode resonators are employed to design compact broadband BPFs [6-10]. A novel high selectivity triple-mode hexagonal BPF with capacitive loading stubs is designed in [6], with the radius of three radial-line stubs just affecting one even-mode resonant frequency while the other two odd-modes remaining unchanged. Another new broadband microstrip BPF is

presented under multiple resonances of an asymmetric ring resonator, reaching a relatively wide 3dB fractional bandwidth of 64% [8]. By stretching the paired stubs close to one-eighth of a wavelength, the first two even-order resonances move down to be quasi-equally located at two sides of the first odd-order resonance, thus forming a bandwidth adjustable BPF. However, all of the above-mentioned filters exhibit unexpected poor upper-stopband performance, since high order harmonic frequencies can hardly be rejected. In [11], a compact wideband BPF whose stopband exceeds to $3.6f_0$ is designed. To achieve a wide stopband, two microstrip short-stubs are loaded to create one transmission zero to avoid the first spurious at the cost of poor in-band performance. Therefore, it is still a great challenge to design a compact broadband BPF with wide stopband and good in-band characteristics.

In this letter, a triple-mode stub-loaded resonator is adopted to design a compact broadband BPF with source-load coupling, as shown in Figure 1. The resonator can generate one odd mode determined by the high impedance line and two even modes flexibly controlled by the loaded stubs at the centre plane in the desired passband. Due to the main path signal counteraction, two transmission zeros T_{z1} , T_{z2} can be created near the passband edge. Owing to the source-load coupling, one transmission zero T_{z3} is created in the upper-stopband and the other four zeros T_{z1} , T_{z2} , T_{z4} , T_{z5} can be slightly adjusted to achieve sharper roll-off skirts and better upper-stopband performance. The proposed broadband filter exhibits good in-band performance, sharp skirt and wide upper-stopband characteristics.

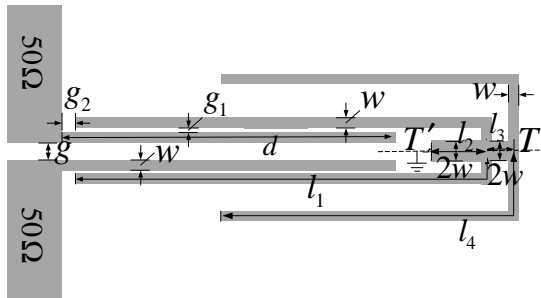


Figure1. Schematic of the tripe-mode broadband BPF with source-load coupling.

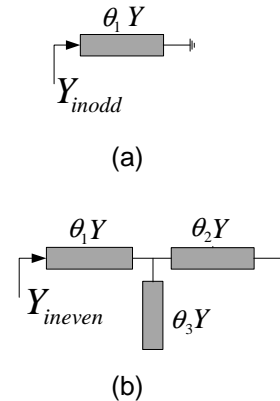


Figure2. (a). odd-mode equivalent circuit. (b). even-mode equivalent circuit.

2. Research Method

The tripe-mode stub-loaded resonator shown in Figure 1 is constructed by a high impedance line with length of $2l_1$ and width of w loaded with one folded stepped-impedance open-circuited stub denoted by lengths (l_3 , $2l_4$) and widths ($2w$, w) and one short-circuited stub with length l_2 and width $2w$ at the central plane. As can be seen, this resonator configuration admits an analysis in terms of even and odd excitations, for the T-T' plane behaves as an electric/magnetic wall for odd/even excitation [12], leading to the approximate transmission line circuit models represented in Figure 2, where θ_1 , θ_2 and θ_3 refer to the electrical lengths of the sections with lengths l_1 , l_2 , and l_3+l_4 , respectively. And Y refers to characteristic admittance of the width w .

Thus the input admittances Y_{inodd} and Y_{ineven} of the odd-mode and even-mode resonators are as follows:

$$Y_{inodd} = -jY \cot \theta_1 \tag{1}$$

$$Y_{ineven} = jY \frac{\tan \theta_1 + \tan \theta_3 - \cot \theta_2}{1 - (\tan \theta_3 - \cot \theta_2) \tan \theta_1} \tag{2}$$

From the conditions $Y_{inodd} = 0$ and $Y_{ineven} = 0$, the resonant frequencies can be extracted as:

$$\cot \theta_1 = 0 \quad (3)$$

$$\tan \theta_1 + \tan \theta_3 - \cot \theta_2 = 0 \quad (4)$$

As expected from formula (3), the resonant frequencies of odd excitation exclusively depend on the high impedance line while having nothing to do with the two loaded stubs, which are determined by formula (5).

$$f_{odd} = \frac{(2n+1)c}{4l_1\sqrt{\epsilon_{eff}}} \quad (5)$$

where c is the speed of light and ϵ_{eff} is equivalent dielectric constant.

The characteristics of the triple-mode stub-loaded resonator are investigated in the case of weak coupling ($d=1mm$). Under the other parameters keeping unchanged, the resonant frequencies with varied l_2 are simulated and shown in Figure 3. The dimensions are chosen as: $l_1=12.9mm$, $l_3=1.3mm$, $l_4=11.1mm$, $g_1=0.1mm$, $g_2=0.22mm$ and $w=0.3mm$. The substrate herein is RT/Duroid 5880 with a thickness of $0.508mm$, permittivity of 2.2 and loss tangent 0.0009. It can be figured out that there are three available resonant frequencies (one odd mode f_{m2} and two even modes f_{m1} , f_{m3}) and four harmonic frequencies (h_{m1} , h_{m2} , h_{m3} , h_{m4}) in the range of 0.1-15GHz. As l_2 increases, f_{m1} and h_{m2} move towards the lower frequency while the others remaining unchanged. Thus, the l_2 is mainly utilized to adjust the first resonant frequency f_{m1} into the desired passband while having no effect on the other two available resonant frequencies (f_{m2} , f_{m3}).

Also the resonant frequencies varied l_3+l_4 are interpreted in Figure 4 when choosing the parameter $l_2=1.9mm$. According to Figure 4, f_{m3} , h_{m1} , h_{m2} and h_{m4} have the same trend of moving downwards while l_3+l_4 is increasing, whereas the first two resonant frequencies f_{m1} , f_{m2} are remaining unchanged.

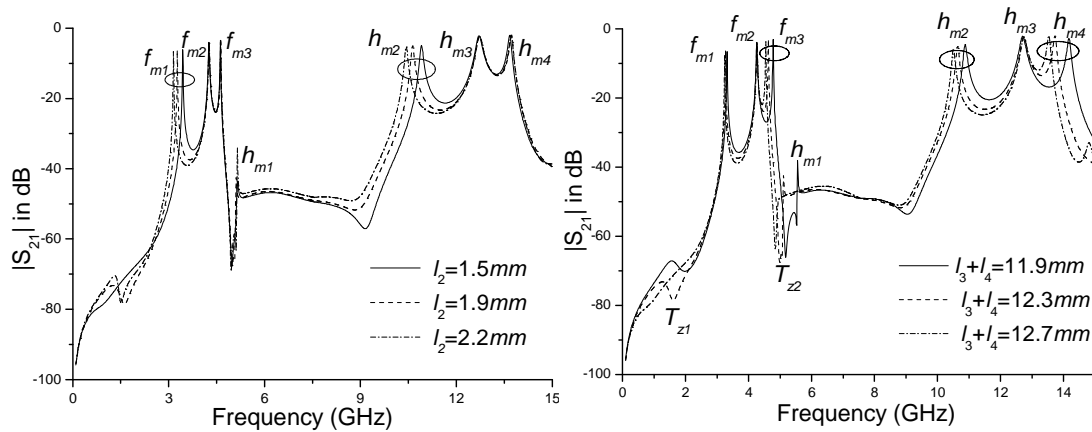


Figure3. Resonant frequencies varied with l_2 . Figure4. Resonant frequencies varied with l_3+l_4 .

In general, the resonant frequency f_{m2} can be adjusted in the centre passband frequency by reasonably choosing the length of the high impedance line, and the other two resonant frequencies f_{m1} , f_{m3} can be adjusted within the desired passband by simply varying the parameters l_2 , l_3 and l_4 . Herein, we may choose the parameters: $l_2=1.9mm$, $l_3=1.3mm$, $l_4=11.1mm$. The first three resonant frequencies are 3.26GHz, 4.29GHz and 4.62GHz,

respectively. If the resonator is properly fed with increased coupling degree [13], the first three resonant modes can be used to make up of a compact broadband BPF.

Under the tight coupling case of $d=10mm$, the simulated insertion losses ($|S_{21}|$ in dB) of the triple-mode broadband BPF with and without source-load coupling (shown in Figure 1 and Figure 5 respectively) are compared in Figure 6. The circuitry dimensions are depicted in Table 1. Two transmission zeros can be created near the passband edges due to the main path signal counteraction, which is explained in [14]. As a result of $f_{1e} < f_{2o} < f_{3e}$ (that is $f_{m1} < f_{m2} < f_{m3}$), the short-circuited stub is used to produce the transmission zero T_{z1} near the lower cut-off frequency, and the location of the transmission zero T_{z2} near the upper cut-off frequency is mainly controlled by the folded open stub.

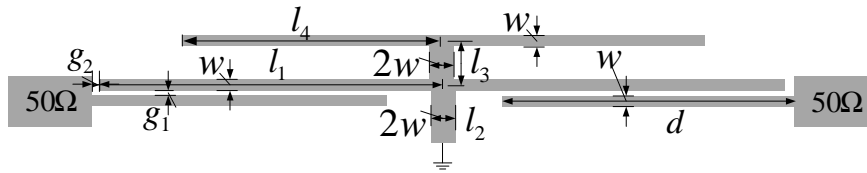


Figure 5. Schematic of the triple-mode broadband BPF without source-load coupling.

Table1. Dimensions of the filter (UNIT: mm).

l_1	l_2	l_3	l_4	w
12.9	1.9	1.3	11.1	0.2
g	g_1	g_2	d	g
0.6	0.1	0.22	10	0.6

As demonstrated in Figure 6, two transmission zeros T_{z4}, T_{z5} are created between two harmonic frequencies h_{m2}, h_{m3} by the folded open stub and the interdigital coupling feeding lines, respectively. Owing to the source-load coupling, T_{z1} is shifted to the lower cut-off frequency and the other three transmission zeros T_{z2}, T_{z4}, T_{z5} can be slightly adjusted to suppress three harmonic frequencies h_{m1}, h_{m2}, h_{m3} . Furthermore, one zero T_{z3} is introduced in the upper-stopband leading to deeper stopband. That is to say, a broadband BPF with sharp skirt, wide upper-stopband and good in-band performance can be achieved by introducing source-load coupling.

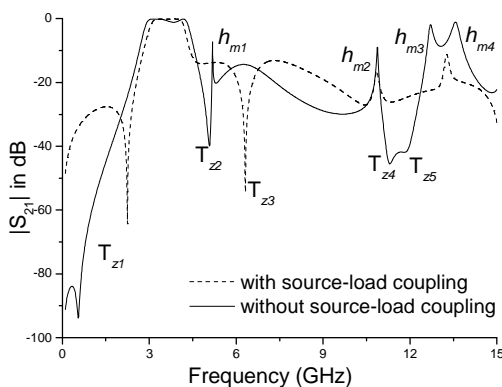


Figure 6. Comparison of the BPF with and without source-load coupling.

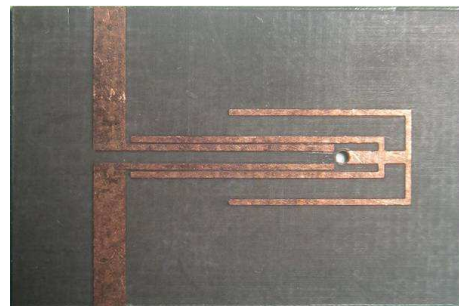


Figure 7. Photograph of the fabricated filter.

3. Results and Analysis

Based on the theories discussed above, the triple-mode broadband BPF with source-load coupling is fabricated on the RT/Duroid 5880 substrate and its photograph is shown in

Figure 7. The filtering performance is measured by Agilent network analyzer N5230A. The measured $|S_{11}|$ in dB and $|S_{21}|$ in dB are shown in Figure 8 (a) and illustrated good agreement with simulated results. The measured 3dB bandwidth is from 3.08 to 4.34 GHz, representing a FBW of 34% at the center frequency of 3.71 GHz. Further, its measured input return loss ($|S_{11}|$ in dB) is less than -20dB. The upper-stopband in experiment is extended up to 13.7GHz with an insertion loss better than -12.5dB. In addition, the measured in-band group delay in Figure 8 (b) is varying from 0.79 to 0.93ns, which is quite small and flat in all the passband. If the feeding lines are ignored, the size of the fabricated filter is only $0.079\lambda_g \times 0.237\lambda_g$ in which λ_g is the guided wavelength of 50Ω microstrip at the center frequency.

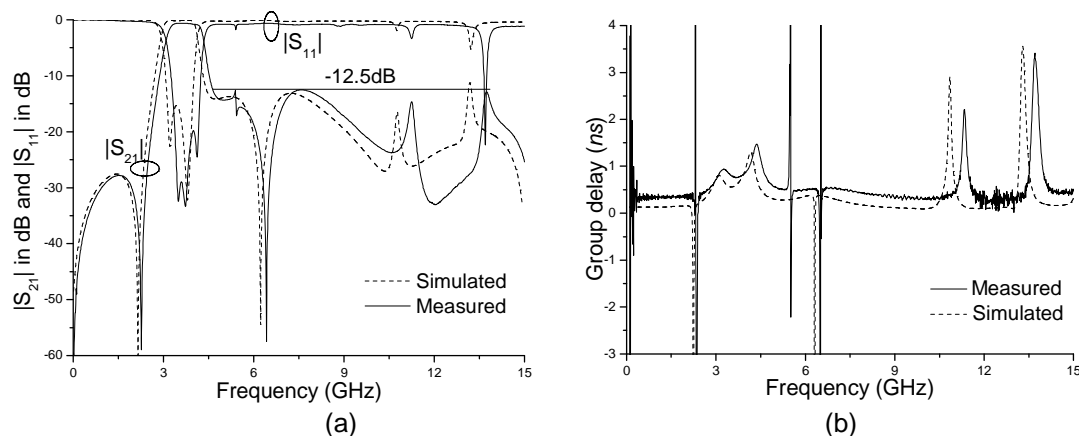


Figure 8. Simulated and measured frequency responses of the fabricated filter. (a). $|S_{21}|$ in dB and $|S_{11}|$ in dB. (b). Group delay.

4. Conclusion

In this letter, a new prototype composed of a triple-mode stub-loaded resonator with source-load coupling has been presented for compact and wide upper-stopband broadband BPF. A fully integrated broadband BPF with a FBW of 34% is simulated, fabricated and measured. Significantly, the filter's upper-stopband in experiment is extended up to $3.7f_0$ with a rejection level better than -12.5dB. Also the rectangular occupying area amounts to only about $0.079\lambda_g \times 0.237\lambda_g$ without considering the feeding lines. With all these advantages above, the broadband BPF is particularly suitable for future broadband applications.

References

- [1]. Srisathit K, Worapishet A, Surakamponorn W. Design of Triple-Mode Ring Resonator for Wideband Microstrip Bandpass Filters. *IEEE Trans. Microw. Theory Tech.*, 2010; 58(11): 2867-2877.
- [2]. Yi-Chyun Chiou, Jen-Tsai Kuo, Cheng E. Broadband Quasi-Chebyshev Bandpass Filters With Multimode Stepped-Impedance Resonators (SIRs). *IEEE Trans. Microw. Theory Tech.* 2008; 54(8): 3352-3358.
- [3]. Chun-Hsiang Chi, Chi-Yang Chang. A wideband bandpass filter with wide upper stopband using stepped-impedance cascaded 180° hybrid rings. *IEEE Microw. Wireless Compon. Lett.* 2007; 17(8):589-591.
- [4]. Sheng Sun, Lei Zhu, Huei-Hsien Tan. A compact wideband bandpass filter using transversal resonator and asymmetrical interdigital coupled lines. *IEEE Microw. Wireless Compon. Lett.* 2008; 18(3):173-175.
- [5]. Yuan Chun Li, Xiu Yin Zhang, Quan Xue. Bandpass Filter Using Discriminating Coupling for Extended Out-of-Band Suppression. *IEEE Microw. Wireless Compon. Lett.*, 2010; 20 (7): 369-371.
- [6]. SG Mo, ZY Yu, L Zhang. Design of triple-mode bandpass filter using improved hexagonal loop resonator. *Progress In Electromagnetics Research*, 2009; 117-125.
- [7]. Kaijun Song, Quan Xue. Novel broadband bandpass filters using Y-shaped dual-mode microstrip resonators. *IEEE Microw. Wireless Compon. Lett.* 2009; 19(9): 548-550.

-
- [8]. Sheng Sun, Lei Zhu. Wideband microstrip ring resonator bandpass filters under multiple resonances. *IEEE Trans. Microw. Theory Tech.* 2007; 55(10).
 - [9]. Ning Yang, Christophe Caloz, Ke Wu, Ning Chen. Broadband and Compact Coupled Coplanar Stripline Filters With Impedance Steps. *IEEE Trans. Microw. Theory Tech.* 2007; 55(12): 2874-2886.
 - [10]. Mehdi Nosrati, Milad Mirzaee. Compact Wideband Microstrip Bandpass Filter Using Quasi-Spiral Loaded Multiple-Mode Resonator. *IEEE Microwave Wireless Component Lett.*, 2010; 20(11): 607-609.
 - [11]. Xun Luo, Jian-Guo Ma, IEEE, Er-Ping Li. Wideband Bandpass Filter With Wide Stopband Using Loaded BCMC Stub and Short-Stub. *IEEE Microw. Wireless Compon. Lett.*, 2011; 21(7): 353-355.
 - [12]. BY Yao, YG Zhou, QS Cao, YC Chen. Compact UWB bandpass filter with improved upper-stopband performance. *IEEE Microw. Wireless Compon. Lett.*, 2009; 19(1):27-29.
 - [13]. R Lei, L Zhu. Compact UWB bandpass filter using stub-loaded multiple-mode resonator," *IEEE Microw. Wireless Compon. Lett.*, 2007;17(1):40-42.
 - [14]. U Rosenberg, S Amari. Novel coupling schemes for microwave resonator filters. *IEEE Trans. Microw. Theory Tech.*, 2002; 50(12): 2896-2902.